

Warmer spring temperatures in temperate deciduous forests advance the timing of tree growth but have little effect on annual woody productivity

Kristina Anderson-Teixeira (✉ TeixeiraK@si.edu)

Smithsonian Conservation Biology Institute <https://orcid.org/0000-0001-8461-9713>

Cameron Dow

Smithsonian Conservation Biology Institute

Albert Kim

Smith College <https://orcid.org/0000-0001-7824-306X>

Loïc D'Orangeville

University of New Brunswick <https://orcid.org/0000-0001-7841-7082>

Erika Gonzalez-Akre

Smithsonian Conservation Biology Institute

Ryan Helcoski

Smithsonian Conservation Biology Institute <https://orcid.org/0000-0003-3579-0121>

Valentine Herrmann

Smithsonian Conservation Biology Institute <https://orcid.org/0000-0002-4519-481X>

Grant Harley

University of Idaho <https://orcid.org/0000-0003-1557-8465>

Justin Maxwell

Indiana University Bloomington <https://orcid.org/0000-0001-9195-3146>

Ian McGregor

Smithsonian Conservation Biology Institute

William McShea

Smithsonian Conservation Biology Institute

Sean McMahon

Smithsonian Tropical Research Institute <https://orcid.org/0000-0001-8302-6908>

Neil Pederson

Harvard University <https://orcid.org/0000-0003-3830-263X>

Alan Tepley

Smithsonian Conservation Biology Institute <https://orcid.org/0000-0002-5701-9613>

Biological Sciences - Article

Keywords:

Posted Date: December 15th, 2021

DOI: <https://doi.org/10.21203/rs.3.rs-1093360/v1>

License:  This work is licensed under a Creative Commons Attribution 4.0 International License.

[Read Full License](#)

Version of Record: A version of this preprint was published at Nature on August 10th, 2022. See the published version at <https://doi.org/10.1038/s41586-022-05092-3>.

1 **Title:** Warmer spring temperatures in temperate deciduous forests advance the timing of tree
2 growth but have little effect on annual woody productivity

3 **Authors:**

4 Cameron Dow^{1,2} (Orcid ID : 0000-0002-8365-598X)

5 Albert Y. Kim^{1,3} (Orcid ID : 0000-0001-7824-306X)

6 Loïc D'Orangeville^{4,5} (Orcid ID : 0000-0001-7841-7082)

7 Erika B. Gonzalez-Akre¹ (Orcid ID : 0000-0001-8305-6672)

8 Ryan Helcoski¹

9 Valentine Herrmann¹ (Orcid ID : 0000-0002-4519-481X)

10 Grant L. Harley⁶ (Orcid ID : 0000-0003-1557-8465)

11 Justin T. Maxwell⁷ (Orcid ID: 0000-0001-9195-3146)

12 Ian R. McGregor^{1,8} (Orcid ID: 0000-0002-5763-021X)

13 William J. McShea¹

14 Sean McMahon^{9,11} (Orcid ID : 0000-0001-8302-6908)

15 Neil Pederson⁴ (Orcid ID : 0000-0003-3830-263X)

16 Alan J. Tepley^{1,10} (Orcid ID : 0000-0002-5701-9613)

17 Kristina J. Anderson-Teixeira^{1,11*} (Orcid ID : 0000-0001-8461-9713)

18 **Author Affiliations:**

19 1. Conservation Ecology Center; Smithsonian Conservation Biology Institute; Front Royal, VA
20 22630, USA

21 2. Department of Forestry and Natural Resources, Purdue University, West Lafayette, Indiana,
22 USA

23 3. Statistical & Data Sciences; Smith College; Northampton, MA 01063, USA

24 4. Harvard Forest, Petersham, MA 01366, USA

25 5. Faculty of Forestry and Environmental Management, University of New Brunswick,
26 Fredericton, NB, E3B 5A3, Canada.

27 6. Department of Earth and Spatial Sciences, University of Idaho, ID 83844, USA

28 7. Department of Geography, Indiana University, Bloomington, IN 47405, USA

29 8. Center for Geospatial Analytics; North Carolina State University; Raleigh, NC 27607, USA

30 9. Smithsonian Environmental Research Center, Edgewater, MD, USA

31 10. Canadian Forest Service, Northern Forestry Centre, Edmonton, Alberta, Canada

32 11. Forest Global Earth Observatory; Smithsonian Tropical Research Institute; Panama,
33 Republic of Panama

34 *corresponding author: teixeirak@si.edu; +1 540 635 6546

35

36 As the climate changes, warmer spring temperatures are causing earlier leaf-out¹⁻⁶ and
37 commencement of net carbon dioxide (CO₂) sequestration^{2,4} in temperate deciduous forests,
38 resulting in a tendency towards increased growing season length^{1,4,5,7-9} and annual CO₂
39 uptake^{2,4,10-14}. However, less is known about how spring temperatures affect tree stem growth,
40 which sequesters carbon (C) in wood that has a long residence time in the ecosystem^{15,16}.
41 Using dendrometer band measurements from 463 trees across two forests, we show that
42 warmer spring temperatures shifted the woody growth of deciduous trees earlier but had no
43 consistent effect on peak growing season length, maximum daily growth rates, or annual
44 growth. The latter finding was confirmed on the centennial scale by 207 tree-ring
45 chronologies from 108 forests across eastern North America, where annual growth was far
46 more sensitive to temperatures during the peak growing season than in the spring. These
47 findings imply that extra CO₂ uptake in years with warmer springs¹⁰⁻¹² is not allocated to
48 long-lived woody biomass, where it could have a substantial and lasting impact on the forest
49 C balance. Rather, contradicting current projections from global C cycle models^{2,3,17,18}, our
50 empirical results imply that warming spring temperatures are unlikely to increase the woody
51 productivity or strengthen the CO₂ sink of temperate deciduous forests.

52 In recent decades, Earth's forests have sequestered ~20% of anthropogenic CO₂ emissions,
53 thereby slowing the pace of atmospheric CO₂ accumulation and climate change^{19,20}. A large
54 portion of this CO₂ sink occurs in temperate deciduous forests, which sequester >300 Tg C yr⁻¹
55 (>30% of the total forest C sink)²¹. The future behavior of this CO₂ sink will play an important
56 yet uncertain role in influencing atmospheric CO₂ and climate change^{20,22}.

57 In temperate deciduous forests, spring warming generally lengthens the period over which
58 trees have photosynthetically active leaves^{1,7-9} and that over which the ecosystem is a net CO₂
59 sink². Current models assume that longer growing seasons lead to increasing annual net CO₂
60 uptake (i.e., net ecosystem exchange, *NEE*)^{2,3,17}. However, recent experimental and observational
61 findings show that annual productivity can be limited by sink factors^{17,23,24}, and that positive
62 effects of warm springs are compensated by negative effects of accumulation of seasonal water
63 deficits³. These studies suggest that warmer spring temperatures may not have the expected
64 positive effect on forest CO₂ sequestration.

65 While responses of leaf phenology and seasonal *NEE* to warming spring temperatures have
66 been documented^{1-4,7-9}, little is known about how the longest-lived component of fixed C in
67 trees, the woody growth, is responding to warming spring temperatures. In fact, we are aware
68 of only one study that has documented stem-growth phenology of temperate deciduous forests
69 over multiple years²⁵. The climate sensitivity of woody growth phenology in temperate
70 deciduous trees and its link to annual growth has never been studied *in-situ* (but see Ref.²⁴ for a
71 controlled sapling experiment).

72 Tree-ring records, which can be used to examine relationships of annual growth to temperature
73 but not to understand growth phenology, reveal that growth of temperate deciduous trees
74 tends to be most sensitive to temperature or potential evapotranspiration between late spring
75 and early summer^{26,27}, with some hints that warmer springs may have a modest positive effect
76 on growth²⁷. Thus, tree-ring evidence does not necessarily align with the finding that warming
77 spring temperatures increase annual forest CO₂ uptake². Characterizing phenological responses

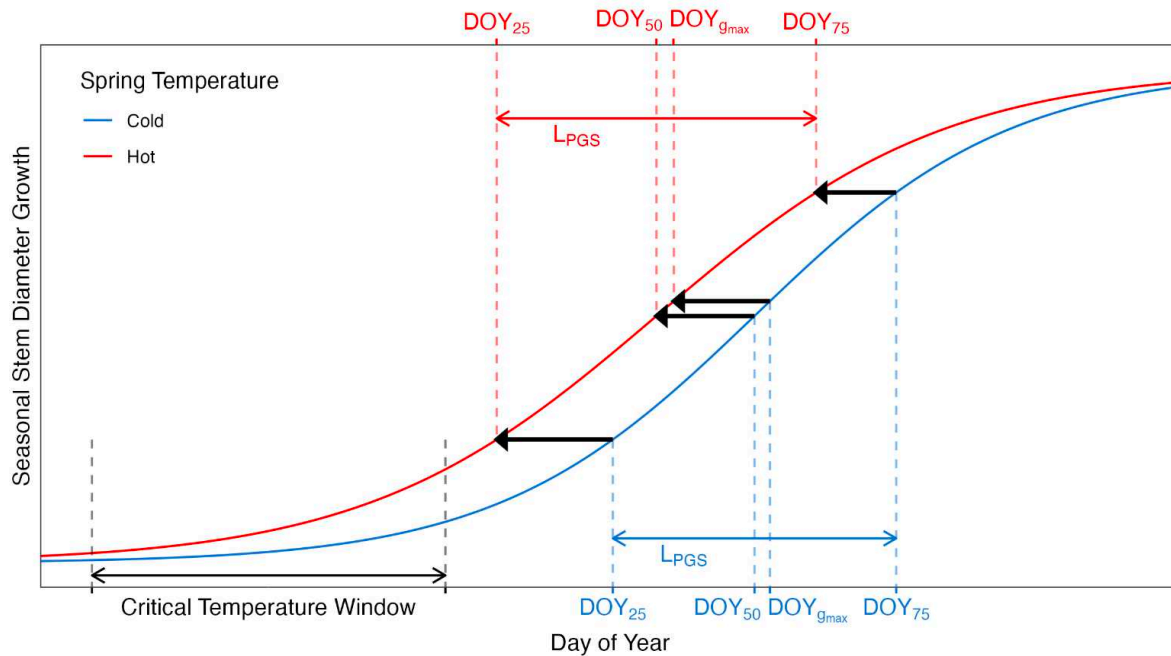
78 of stem growth to warming spring temperatures is critical to bridging this conceptual
79 disconnect and understanding how forest biomass growth is likely to change as the climate
80 warms.

81 Here, we evaluate how early spring temperatures affect stem growth phenology, growth rates,
82 and annual growth of temperate deciduous trees across eastern North America. To test whether
83 warmer springs extend the period of stem growth, we used dendrometer band measurements
84 on 463 trees across two mid-latitude forests. To test whether spring temperatures consistently
85 increased annual growth, we analyzed 207 tree-ring chronologies from 108 forests.

86 **Dendrometer band analysis**

87 Using dendrometer band measurements taken throughout multiple growing seasons at the
88 Smithsonian Conservation Biology Institute (SCBI; Virginia, USA; $n = 123$ trees from 2011-2020)
89 and Harvard Forest (Massachusetts, USA; $n = 340$ trees from 1998-2003), we fit a logistic growth
90 model²⁸ to determine the days of year (DOY) when 25, 50, and 75% annual growth were
91 achieved (DOY_{25} , DOY_{50} , DOY_{75}), peak growing season length ($L_{pgs} = DOY_{75} - DOY_{25}$), the
92 maximum daily growth rates (g_{max}) and the DOY on which it occurred ($DOY_{g_{max}}$), and total
93 annual increment in diameter at breast height (ΔDBH ; Fig. 1). This analysis was performed
94 separately for ring- and diffuse-porous species, which differ in growth phenology²⁵. These stem-
95 growth milestones were compared to canopy foliage phenology (measured at ecosystem level
96 via remote sensing).

(a)

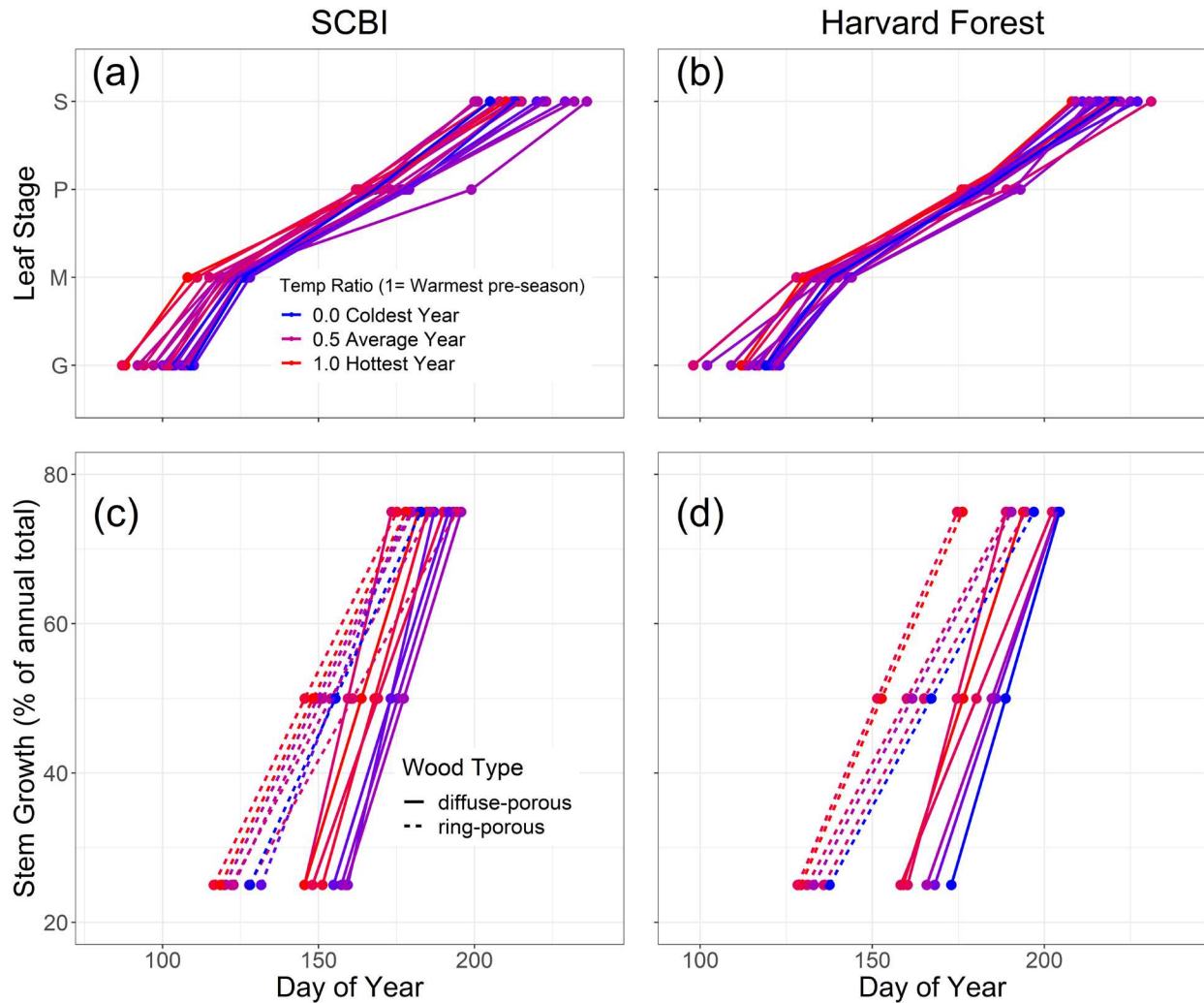


(b)

Variable	Definition	Response to warmer spring T			
		SCBI		Harvard Forest	
		RP	DP	RP	DP
Timing of growth					
DOY_{25}	day of year at which 25% of growth is achieved	↓	↓	↓	↓
DOY_{50}	day of year at which 50% of growth is achieved	↓	↓	↓	↓
DOY_{75}	day of year at which 75% of growth is achieved	↓	↓	↓	↓
$DOY_{g_{max}}$	day of year of max growth rate	↓	↓	↓	↓
L_{PGS}	peak growing season length ($DOY_{75} - DOY_{25}$)	↑	-	↓	↑
Daily growth rate					
g_{max}	maximum daily growth rate	-	-	↑	↓
Annual growth					
ΔDBH	annual growth	-	-	-	-
RWI	ring width index from tree-ring chronologies	mixed	mixed	-	mixed

98 **Figure 1 | Summary of temperate deciduous tree growth responses to warmer spring temperatures.** (a)
 99 Schematic illustrating parameters of interest and summarizing how each responds to warmer maximum
 100 temperatures during a 'critical temperature window', defined as the period with the strongest control
 101 over DOY_{25} ; (b) Variable definitions and summary of responses to warmer spring temperatures at two
 102 temperate forests – Smithsonian Conservation Biology Institute (SCBI) and Harvard Forest – and for two
 103 groups of broadleaf deciduous species (RP=ring porous; DP=diffuse porous), where up and down arrows
 104 indicate significant increases and decreases, respectively, '-' indicates no significant correlation, and
 105 'mixed' indicates a mix of significant and non-significant correlations, often in different directions.

106 Growth milestones for both canopy foliage phenology and stem growth occurred 6-10 days
107 earlier, on average, at SCBI than at Harvard Forest (Fig. 2, Extended Data Table 2). Consistent
108 with the results of Ref²⁵, ring-porous species began growing earlier, reaching the DOY_{25}
109 benchmark earlier (by 31 days at SCBI and 32 at Harvard Forest), and their growth was spread
110 over a longer growing season (average L_{PGS} 21 and 19 days longer at SCBI and Harvard Forest,
111 respectively; Fig. 2, Extended Data Figure 2, Extended Data Table 2). Peak growing season
112 length was similar across sites, with L_{PGS} being, on average, only two days longer at SCBI for
113 ring-porous species and less than one day longer for diffuse-porous species (Extended Data
114 Table 2).



116 **Figure 2 | Foliage (a,b) and stem growth (c,d) phenology at the Smithsonian Conservation Biology**
 117 **Institute (a,c) and Harvard Forest (b,d).** Panels (a-b) show ecosystem-level canopy foliage phenology
 118 from 2001-2018, obtained from the MODIS Global Vegetation Phenology product (MCD12Q2.006), where
 119 G = Greenup, M=Mid-greenup, P=peak, and S=Senescence (i.e., beginning of green-down). Panels (c-d)
 120 show the dates at which stem growth milestones were achieved, on average, for sampled populations of
 121 ring-porous and diffuse-porous trees at SCBI (2011-2020) and Harvard Forest (1998-2003). Mean
 122 temperature was calculated for each wood-type/site combination over the respective critical T_{max}
 123 window, then turned into a ratio and assigned a color on a gradient where the coldest year in the sample
 124 is blue and the warmest is red.

125

126 Both MODIS-derived canopy foliage phenology and dendrometer band measurements of stem
 127 growth phenology generally shifted backwards as spring temperatures increased (Fig. 2,
 128 Extended Data Figures 4-5). We found a consistent effect of temperature (T_{max} or T_{min})

129 throughout the spring, but the strongest effects on stem-growth phenology were found using
130 T_{max} during a critical temperature window (CTW). CTW was identified by measuring the
131 correlation between all combinations of weekly T_{max} and DOY_{25} from January 1 to mean DOY_{25}
132 for each xylem porosity-site combination (Extended Data Figure 3). The CTW was defined as
133 the week(s) which had the strongest correlation with DOY_{25} .

134 For ring- and diffuse- porous species at both sites, warmer T_{max} in the CTW resulted in earlier
135 achievement of phenological milestones. Consistent with findings from previous studies³⁰, leaf
136 phenological milestones advanced at both sites (Fig. 2a-b, Extended Data Table 2), with greenup
137 (DOY when EVI2 first crossed 15% of the segment EVI2 amplitude) advancing 4.5 days/°C at
138 SCBI (p=0.001) and 2.4 days/ °C at Harvard Forest (p=0.1). Similarly, at both sites, the stem
139 growth milestones DOY_{25} , DOY_{50} , DOY_{75} , and $DOY_{g_{max}}$ all decreased with mean T_{max} during the
140 critical temperature window (Figs. 1, 2c-d; Extended Data Figures 4-5). Specifically, DOY_{25} ,
141 DOY_{50} , and DOY_{75} advanced 1.1-1.9 days/ °C for ring-porous species and 3.5-3.6 days/ °C for
142 diffuse-porous species at SCBI, and 2.8-7.2 days/ °C for ring-porous species and 6.6-7.9 days/ °C
143 for diffuse-porous species at Harvard Forest (Extended Data Table 2).

144 Whereas the length of time between canopy greenup and senescence (*i.e.*, the day when
145 greenness dropped below 90% of its peak) increased in years with warmer temperatures during
146 the critical temperature window compared to those with cooler temperatures (Fig. 2a-b), there
147 was no consistent lengthening of L_{PGS} (Fig. 1, Extended Data Figures 4-5).

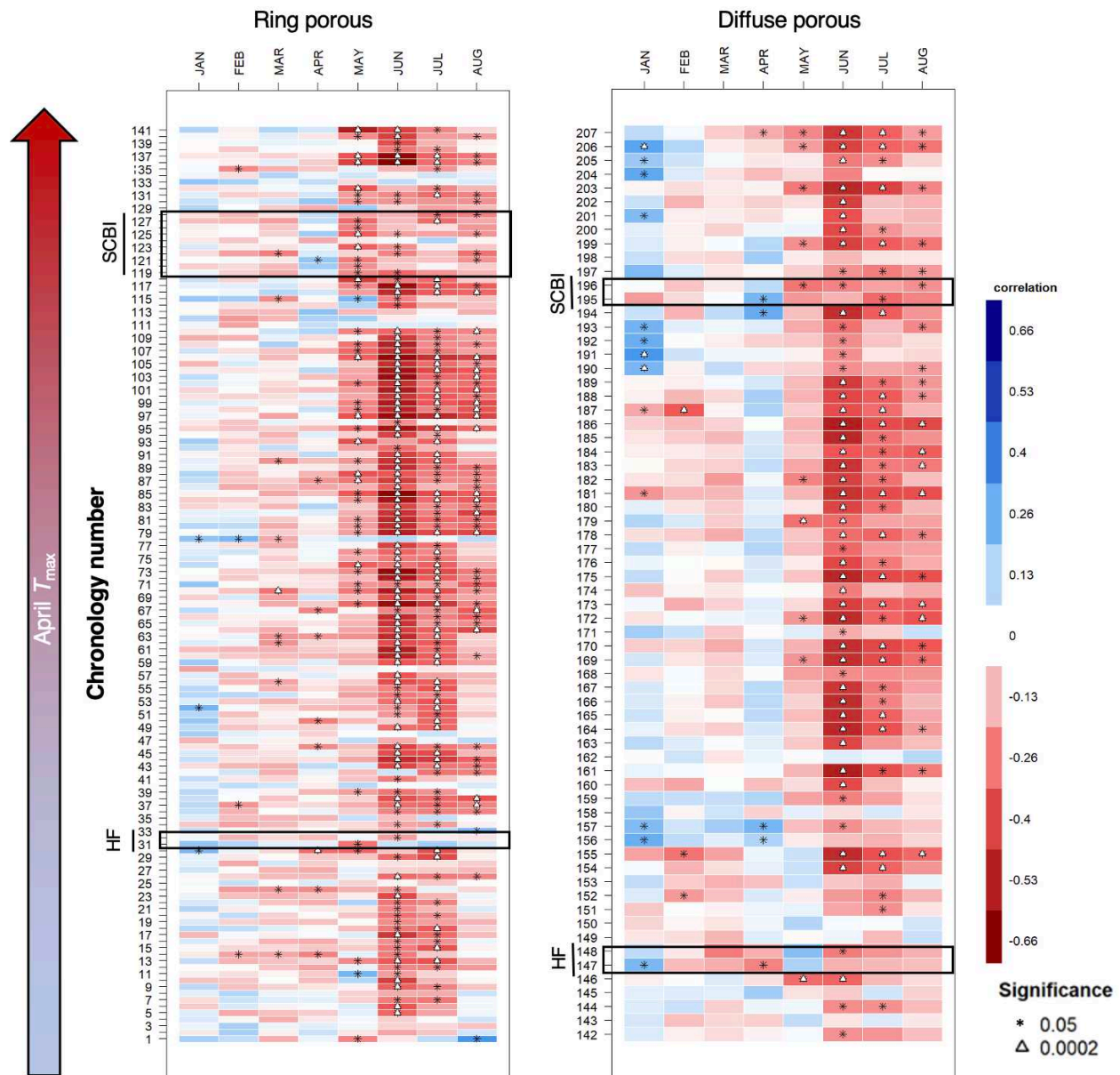
148 In contrast to the pronounced effects of T_{max} on the timing of growth, its effects on g_{max} and
149 ΔDBH were weak and inconsistent (Figs. 1, Extended Data Figures 4-5). Specifically, g_{max} ,

150 which occurred very close to DOY_{50} (on $DOY_{g,max}$; Extended Data Table 2), displayed either no
151 relationship to mean T_{max} during the critical temperature window (SCBI), or extremely small
152 changes in opposite directions for ring- and diffuse- porous species (Harvard Forest). ΔDBH
153 displayed no relationship with mean T_{max} during the critical temperature window (Extended
154 Data Figure 4).

155 **Tree-ring analysis**

156 To understand how annual growth increments have responded to spring temperatures at the
157 centennial scale, we analyzed tree-ring chronologies of 12 species at SCBI²⁷ and 4 species at
158 Harvard Forest (Extended Data Table 1), along with an additional 191 chronologies from 106
159 sites (Fig. 3; Extended Data Figure 1; Extended Data Table 3)²⁶. In total, our analysis included
160 207 chronologies representing 24 broadleaf species at 108 sites distributed from Alabama (Lat =
161 34.35) to Michigan (Lat = 45.56) and spanning a 15 °C range in April T_{max} . Across all
162 chronologies, the standardized ring-width index (RWI) was significantly (at $p \leq 0.05$) positively
163 correlated with April T_{max} for only 2% of chronologies: 1 of 142 ring-porous and 4 of 66 diffuse-
164 porous species-site combinations (Extended Data Table 3). In contrast, RWI was frequently
165 negatively correlated with T_{max} during peak growing season months (May-August), with
166 significant correlations for 52% (May: 45/141, Jun: 107/141, Jul: 91/141, Aug: 53/141) and 46%
167 (May: 10/66, Jun: 52/66, Jul: 36/66, Aug: 23/66) of species-site-month combinations for ring-
168 porous and diffuse-porous species, respectively. T_{min} generally exhibited weaker relationships to
169 annual growth than T_{max} , with few significant correlations between spring T_{min} and RWI
170 (Extended Data Figure 6).

171 To test whether the negative effect of summer temperatures might offset an enhancement of
172 growth by warmer spring temperatures, we tested for the joint effects of April and June-July
173 T_{max} on RWI. Results were qualitatively similar to the univariate correlations (Fig. 3), with
174 significant (at $p = 0.05$) positive correlations to April T_{max} for only 4% of chronologies and
175 significant negative correlations with June-July T_{max} for 77% of chronologies, supporting that
176 summer temperatures were the more important driver of annual stem growth (Extended Data
177 Table 3).



179 **Figure 3 | Sensitivity of annual growth, as derived from tree-rings, to monthly mean maximum**
 180 **temperatures (T_{max}), for 207 chronologies from 108 sites across eastern North America (Extended Data**
 181 **Figure 1). Colors indicate the correlation between monthly T_{max} and a dimensionless ring width index**
 182 **(RWI) derived from the multiple trees that form each chronology and emphasizing interannual variability**
 183 **associated with climate. Chronologies are grouped by xylem porosity and ordered by mean April T_{max} .**
 184 **Plots are annotated to highlight records from our two focal sites, the Smithsonian Conservation Biology**
 185 **Institute (SCBI) and Harvard Forest (HF) (Extended Data Table 1). Species analyzed and numbers of**
 186 **significant correlations to T_{max} are summarized in Extended Data Table 3, and chronology details are**
 187 **given in SI Table 1.**

188 **Discussion**

189 Together, our results demonstrate that warmer spring temperatures in the temperate deciduous
190 forests of eastern North America advance the phenology of tree stem growth but have little
191 effect on annual woody productivity (Figs. 1- 3). The observed phenological advance in the start
192 of stem growth under warmer springs parallels phenological advances observed for canopy
193 foliage (Fig. 2a-b)^{2,4,5} and *NEE*^{2,4}. However, inconsistent with the concept that an earlier start to
194 growth would increase annual woody productivity, we demonstrate that warmer springs
195 hasten the cessation of stem expansion and thereby have negligible effect on total annual
196 growth for most species and locations (Fig. 3). Our observations suggest that the cessation of
197 rapid stem expansion, which occurs mid-summer near the time of peak canopy greenness
198 (Extended Data Figure 2)⁴, is likely driven by cues other than photosynthate limitation, such as
199 daylength or sink limitation, which also play an important role in autumn leaf senescence^{17,23,31}.
200 Our tree-ring analysis (Fig. 3) demonstrates that the primary effect of warming temperatures on
201 annual tree growth is not an augmentation through an earlier start to growth, but rather a
202 reduction associated to drought stress during the peak growing season²⁶. Warm springs may
203 also amplify summer drought stress in some times and places, effectively canceling out any
204 positive effects of an extended growing period^{3,32}; however, spring temperatures and summer
205 Standardized Precipitation Evapotranspiration Index³³ were uncorrelated within our
206 dendrometer band analysis, implying that the effects of warm spring temperatures on growth
207 phenology elucidated here (Fig. 1) were not attributable to summer drought.

208 Our finding that interannual variation in woody growth is more strongly linked to conditions
209 during the peak growing season than to growing season length aligns with parallel findings for
210 *NEE*^{13,14}. However, there is also a disconnect with findings that *NEE* is at least modestly greater
211 in years with warm springs² or long growing seasons^{4,13,14}. Warming advances spring phenology
212 and may advance or delay autumn senescence depending on timing of warming and water
213 availability^{12,34,35}, with delays more common across eastern North America,²⁻⁴ implying that
214 warming temperatures are lengthening the period from peak stem growth to the cessation of
215 CO₂ uptake by the ecosystem. We show that the extra C fixation in years with warm springs
216 does not substantially augment woody growth, but it remains unclear how it is allocated within
217 the ecosystem. There are two main possibilities, which hold contrasting implications for the
218 response of forest C balance to rising spring temperatures.

219 One possibility is that extra photosynthate in years with warm springs may be allocated to
220 woody growth without affecting diameter growth in the current year. It is theoretically possible
221 that extra C is allocated to cell wall thickening, a process that lags behind stem expansion³⁶, or
222 to a thicker layer of higher-density latewood, resulting in formation of more C-dense wood in
223 years with warm springs. However, existing evidence indicates that warm springs have a
224 neutral or negative effect on latewood width³⁷⁻³⁹, which is more strongly controlled by summer
225 drought stress^{37,38}, suggesting that a positive effect of warm springs on the total C content of
226 annual rings is unlikely. Extra C could also be saved within trees as non-structural
227 carbohydrates and used towards growth the following year^{40,41}, potentially including an earlier
228 start to growth³¹. Extension of our tree-ring analysis revealed weak correlation between April
229 T_{max} and growth the following year (sig. pos. correlations for 5/142 RP and 3/66 DP species-site

230 combinations, Fig. Extended Data Figure 7), although predominantly positive (non-significant)
231 correlations in RP species suggests that this dynamic may weakly influence their annual
232 growth. Thus, warm springs are unlikely to provide substantial, sustained C sinks under
233 warming spring temperatures.

234 A second possibility is that any additional C fixed during years with warm springs may be
235 allocated to plant functions other than stem growth, including respiration, reproduction, and
236 production of foliage, roots²⁴, or root exudates. Much of this C would have a relatively short
237 residence time within the ecosystem, and C loss through fall or winter respiration may offset
238 gains from an earlier spring^{3,42}. However, C allocated to nonstructural carbohydrates or
239 relatively short-lived plant tissues would typically remain in the ecosystem beyond the end of
240 the year⁴⁰, such that the long-term effect of warm springs on the forest C balance would not be
241 captured in analyses of interannual variation^{2,13,14}. Studies within or including the temperate
242 deciduous biome that examined long-term trends in growing season length and ecosystem C
243 uptake^{2,4,10,11} – as opposed to their interannual variation – showed increasing trends in both
244 variables, suggesting that the C not allocated to woody productivity within the current year has
245 a multi-year residence time within the ecosystem. However, given our finding that warm
246 springs do not significantly enhance woody productivity, this C is likely to have a relatively
247 short residence time within the ecosystem.

248 Thus, a distinction between interannual variation and directional change may be critical when
249 considering how directional climate change is likely to affect tree growth and ecosystem C
250 dynamics. As discussed above, temporal lags between C uptake and release imply that the full

251 effects of warm spring temperatures on forest woody productivity and C cycling are unlikely to
252 be apparent in analyses of interannual variation (including this analysis)⁴³. Moreover,
253 acclimation of trees to warming temperatures⁴⁴ and, on longer time scales, species adaptations
254 and shifts in community composition⁴⁵ are likely to alter the phenology of forest C cycling. If we
255 look across spatial gradients where the latter have had time to play out, we see that warmer
256 spring temperatures are associated with earlier leaf-out⁶ and longer growing seasons, which in
257 turn are correlated with greater tree growth⁴⁶, woody productivity⁴⁷, and *NEE*⁴⁸. Thus,
258 warming spring temperatures are expected to increase the biophysical potential for annual tree
259 growth, but that potential is not being realized on an interannual time frame.

260 As climate change accelerates and spring temperatures become increasingly warmer, growing
261 seasons will start earlier; however, barring rapid acclimation of forests to the warming
262 conditions, an earlier onset of growth in the spring is unlikely to provide the sustained increase
263 in CO₂ sequestration and ensuing negative climate change feedback that is anticipated in most
264 climate forecasting models^{2,3,17,18}. Rather, the dominant effect of rising temperatures on forest
265 woody productivity will be a negative effect of high summer temperatures, which constitutes a
266 positive feedback to climate change.

267 **Methods**

268 **Dendrometer band analysis**

269 Dendrometer band measurements were collected at SCBI⁴⁹ and Harvard Forest^{4,25}, both part of
270 the Forest Global Earth Observatory (ForestGEO)^{50,51}. SCBI (38.8935° N, 78.1454° W; elevation

271 273–338 m.a.s.l.) is located in the Blue Ridge Mountains at the northern end of Shenandoah
272 National Park, 5 km south of Front Royal, Virginia. The forest is secondary and mixed age,
273 having established in the mid-19th century after conversion from agricultural fields⁴⁹. Dominant
274 canopy species within the 25.6 ha ForestGEO plot include tulip poplar (*Liriodendron tulipifera* L.),
275 oaks (*Quercus spp.*), and hickories (*Carya spp.*)²⁷. The climate is humid temperate, with 1950-2019
276 mean annual precipitation of 1018 mm and temperatures averaging 1° C in January and 24° C in
277 July⁴⁶.

278 Harvard Forest (42.5388° N, 72.1755° W, 340-368 m.a.s.l.) is located near the central
279 Massachusetts town of Petersham. The forest is secondary and mixed age, having re-established
280 around the beginning of the 20th century following agricultural use and significant hurricane
281 damage in 1938. Dominant species within the 35 ha ForestGEO plot are hemlock (*Tsuga*
282 *canadensis* (L.) Carrière), oak (*Quercus spp.*) and red maple (*Acer rubrum* L.). The climate is
283 temperate continental, with 1950-2019 mean annual precipitation of 1104 mm and temperatures
284 averaging -5° C in January and 22° C in July⁴⁶.

285 Metal dendrometer bands were installed on 941 trees within the SCBI and Harvard Forest
286 ForestGEO plots. Bands were placed on dominant species, including two diffuse- and two ring-
287 porous species at SCBI and eight diffuse- and three ring-porous species at Harvard Forest
288 (Extended Data Table 1). Bands were measured with a digital caliper approximately every 1-2
289 weeks within the growing season from 2011-2020 at SCBI and 1998-2003 at Harvard Forest. The
290 number of bands measured at each site fluctuated slightly as trees were added or dropped from
291 the census (e.g., because of tree mortality). Across years, the number of bands sampled

292 averaged 129 (range: 91-138) at SCBI and 717 (range: 700-755) at Harvard Forest. In total, our
293 analysis included 2459 tree-years (Extended Data Table 1).

294 Measurements were timed to begin before the beginning of spring growth and to continue
295 through the cessation of growth in the fall. At SCBI, the median start date was April 14, which
296 was adjusted forward when early leaf-out of understory vegetation was observed, with the
297 earliest start date being March 30 (in 2020). Measurements were continued through to fall leaf
298 senescence, with the median end date being October 17 and the latest end date November 26
299 (2012). Timing of measurements at Harvard Forest were similar, with the median start date of
300 April 23 and median end date of October 30. 1998 was an anomalous year where initial
301 measurements were taken on January 5, but not taken again until April 15. The latest end date
302 was November 11, 2002.

303 The raw dendrometer band data were manually inspected before analysis. We screened the
304 data for three classes of errors. First, when a measurement was drastically different from
305 previous and following measurements, it was assumed to be a human error and the datapoint
306 was removed. Second, when measurements remained essentially unchanged for several
307 readings, followed by a sudden jump then return to a normal growth pattern, this was assumed
308 to be a case where the band was stuck on the tree bark and then released. In these cases, the full
309 annual record for the tree was removed. Third, data points that deviated substantially from
310 normal growth patterns, but for unknown causes, were removed. If a majority of the data points
311 fell into this class within a tree-year, the entire year was removed from the analysis.

312 We fit a five-parameter logistic growth model²⁸ to dendrometer band data from each tree-year
313 to define phenological dates and growth rates (Fig. 1). In particular, we model the observed
314 diameter at breast height (DBH) on a given day of the year (DOY; *i.e.*, julian days) as:

$$315 \quad DBH = L + \frac{K - L}{1 + 1/\theta \cdot \exp[-r(DOY - DOY_{ip})/\theta]}^\theta$$

316 Here, L and K are lower and upper asymptotes of the model, corresponding to DBH at the
317 beginning and end of the year, respectively. DOY_{ip} is the day of year where the inflection point
318 in growth rate occurs, r shapes the slope of the curve at the inflection point, and θ is a tuning
319 parameter controlling the slope of the curve toward the upper asymptote. The DOY on which
320 maximum growth occurs, DOY_{gmax} (Fig. 1), occurs on DOY_{ip} when $\theta = 1$. The model was fit in R
321 v4.0 using the functions developed in the *Rdendrom* package²⁸. These functions take the time-
322 series of manual dendrometer band measurements and return maximum-likelihood optimized
323 values of the above five parameters that best predict DBH for each day of year. We then
324 modeled DBH using these optimal parameter values in our logistic growth model and extracted
325 the intra-annual growth variables of interest (Fig. 1).

326 After fitting the growth model, we removed tree-years with poor fits. Models were judged to be
327 poorly fit if certain modeled growth characteristics fell outside of the logical range. Modeled fits
328 for tree-years were removed under five conditions: (1) single day growth rates were ≥ 2
329 standard deviations away from the mean for each wood-type (SCBI = 2, Harvard Forest = 34);
330 (2) DOY_{ip} was ≥ 2 standard deviations away from the mean for its xylem architecture group,
331 year, and site (SCBI = 53, Harvard Forest = 106); (3) tree-years with small or negligible total

332 growth ($\Delta DBH \leq 0.02$ mm; SCBI = 0, Harvard Forest = 66); (4) model fit predicted total yearly
333 growth to take longer than 365 days, indicating poor model fit (SCBI = 150, Harvard Forest =
334 199); (5) models with unexplained sharp spikes in growth rate (SCBI = 0, Harvard Forest = 3);
335 and (6) poorly fit models that did not meet any of the above criteria (SCBI = 2, Harvard Forest =
336 0). At Harvard Forest the tag years removed through this method were proportional to the
337 original sample size, indicating that no species or size class was disproportionately removed
338 compared to others. At SCBI, a higher proportion of ring-porous trees were removed, the
339 majority falling under condition 4.

340 Canopy foliage phenology data for the years 2001-2018 were extracted for SCBI and Harvard
341 Forest from the MCD12Q2 V6 Land Cover Dynamics product (a.k.a. MODIS Global Vegetation
342 Phenology product)⁵² via Google Earth Engine. Extracted pixels were those containing the
343 NEON tower at each site. Using daily MODIS 2-band Enhanced Vegetation Index data (EVI2) at
344 a spatial resolution of 500m, the product yields the timing of phenometrics (vegetation
345 phenology) over each year, including timing of greenup, midgreenup, and senescence as used
346 in this study.

347 For the dendrometer band and leaf phenology analyses, climate data corresponding to the
348 measurement periods were obtained from local weather stations at each focal site. For SCBI,
349 weather data were obtained from a meteorological tower adjacent to the ForestGEO plot, via the
350 ForestGEO Climate Data Portal v1.0 (<https://forestgeo.github.io/Climate/>)⁵³. The R package
351 *climpact* (see www.climpact-sci.org)⁵⁴ was used to plot temperatures for visual inspection and to
352 identify readings that were >3 standard deviations away from yearly means, which were

353 labeled as outliers and removed from the dataset. Gaps in the SCBI meteorological tower data
354 were subsequently filled using temperature readings obtained from a National Center for
355 Environmental Information (NCEI) weather station located in Front Royal, Virginia
356 (<https://www.ncdc.noaa.gov/cdo-web/datasets/GHCND/stations/GHCND:USC00443229/detail>).

357 Daily temperature records for Harvard Forest, which had already been gap-filled based on
358 other local records, were obtained from the Harvard Forest weather station^{55,56}. For each site, we
359 used records of daily maximum (T_{max}) and minimum temperatures (T_{min}).

360 The critical temperature window (CTW, Fig. 1), defined as the period over which T_{max} was
361 most strongly correlated with DOY_{25} , was determined using the R package *climwin*⁵⁷. This
362 package tests the correlation between one or more predictor climate variable and a biological
363 outcome variable over all consecutive time windows within a specified time-frame. It does so
364 by reporting the correlation and $\Delta AICc$, the difference in Akaike Information Criterion corrected
365 for small sample size relative to a null model for each window. Here, we tested for correlation
366 between temperature predictor variables (T_{max} , T_{min}) and biological outcome variable DOY_{25}
367 over the time-frame from January 1 to the mean DOY_{25} for the species group (by xylem porosity)
368 and site (Extended Data Table 2). The time period yielding the lowest $\Delta AICc$ was selected as the
369 CTW. Because T_{max} proved to have a generally stronger influence over DOY_{25} and other growth
370 parameters, we focused on this variable in our ultimate model, as opposed to T_{min} . We defined
371 CTW for DOY_{25} , as opposed to other growth phenology parameters, because spring
372 temperatures should have the most direct influence on this variable.

373 To ensure that patterns were robust under an alternative definition of CTW, and to parallel the
374 monthly time windows used in our tree-ring analysis (detailed below; Fig. 3, Extended Data
375 Figure 6-7), we also ran analyses where we fixed the CTW to be the month of April. This was
376 consistent with the periods identified by *climwin* for ring- and diffuse-porous species groups at
377 both sites, all of which included all or part of April (Extended Data Table 2).

378 Correlation between the dendrometer band-derived growth parameters (DOY_{25} , DOY_{50} , DOY_{75} ,
379 $DOY_{g_{max}}$, L_{PGS} , g_{max} , and ΔDBH), Fig. 1) and spring temperatures were assessed using a linear
380 mixed model in a hierarchical Bayesian framework. Analyses were run for both T_{max} and T_{min} ,
381 with qualitatively similar results, but we present only results for T_{max} , which had overall
382 stronger correlation with growth parameters. Mixed effects models were used to test the
383 response of growth phenology variables to fixed effects of xylem porosity and mean T_{max} (or
384 T_{min}) during the CTW, along with random effects of species and of individual tree. We ran
385 separate models for each species group at each site, and for the response of all growth
386 phenology variables to T_{max} (or T_{min}). This mixed-effect model was run within a hierarchical
387 Bayesian framework and fit using the `rstanarm` R interface to the Stan programming
388 language^{58,59}. In all cases unless otherwise specified, all prior distributions are set to be the
389 weakly informative defaults.

390 To rule out the possibility that observed patterns were strongly influenced by summer drought,
391 we examined the relationship between spring temperatures and summer Standardized
392 Precipitation Evapotranspiration Index³³. The latter was obtained from the ForestGEO Climate
393 Data Portal v1.0 (<https://forestgeo.github.io/Climate/>)^{53,60,61}. Linear models were run with 4-, 6-,

394 and 12-month SPEI values of June, July, and August vs April T_{max} to determine if warm spring
395 temperatures lead to greater summer drought stress. No significant correlations were found (all
396 $p > 0.05$).

397 **Tree-ring analysis**

398 We analyzed tree-ring records for 108 sites, including our focal sites. All cores had been
399 previously collected, cross-dated, and measured using standard collection and processing
400 methodologies⁶².

401 Dominant tree species were cored at both SCBI^{27,49} and Harvard Forest^{4,63,64} following sampling
402 designs that covered a broad range of DBH. We analyzed records for the ring- and diffuse-
403 porous species at each site (Extended Data Table 1), but excluded species with other xylem
404 architectures (*Juglans nigra* L. at SCBI, *Tsuga canadensis* at Harvard Forest). We studied a total of
405 976 cores which included 12 species at SCBI and 4 species at Harvard Forest (Extended Data
406 Table 1).

407 The tree-ring records from our focal sites were complemented with a much larger collection
408 spanning 106 deciduous and mixed forest sites in Eastern North America^{26,65}. Again, records
409 were limited to broadleaf deciduous species with clearly defined xylem porosity (*i.e.*, excluding
410 semi-ring porous).

411 For each species-site combination, we converted tree-ring records into the dimensionless RWI to
412 emphasize interannual variability associated with climate.⁶⁶ A 2/3rds n spline was applied to
413 each core using ARSTAN to produce standardized ring-width series; n is the number of years in

414 each series^{66,67}. An adaptive power transformation, a process that also stabilises the variance
415 over time⁶⁸, was used to minimize the influence of outliers in all series. Low series replication,
416 often in the earliest portions of a chronology collection, can also inflate the variance of tree-ring
417 records⁶⁹. The 1/3rds spline method was chosen when replication in the inner portion of each
418 chronology (ca. inner 30–50 yr of each record depending on full chronology length) was less
419 than three trees. When replication was greater than $n = 3$ trees, we used the average correlation
420 between raw ring-width series (rbar) method. The robust biweight mean chronology (RWI) for
421 each species-site combination was calculated from the ring-width indices following variance
422 stabilisation⁶⁷. We defined chronology start year (Extended Data Table 1) as the year where
423 subsample signal strength (SSS) passed a threshold of $SSS = 0.8$, or where $\geq 80\%$ of the
424 population signal was captured in the chronology.

425 For the analysis of correlation between RWI and climate variables, we obtained monthly T_{max}
426 and T_{min} data for 1901-2019 from CRU v.4.04.⁷⁰ Correlations between monthly climate and *RWI*
427 were assessed using 'dplr'⁷¹ and 'bootRes'⁷² in R v 4.0 (R Core Team, 2020), which correlated
428 functions and bootstrapped confidence intervals for these relationships⁷³. We analyzed these
429 correlations for January through September of the current year (presented in Fig. 3, Extended
430 Data Figure 6). To test for potential lag effects of spring temperatures on growth the following
431 year, we also ran a version of the analysis extending back to include climate of every month of
432 the previous year (Extended Data Figure 7). Correlations and significance levels for months
433 April-August are given in SI Table 1.

434 We used a multivariate model to test for joint effects of April and summer T_{max} on RWI. We
435 began by testing univariate correlations of T_{max} over three summer windows: June, June-July,
436 and May-August. Having determined that, among these, June-July explained the most
437 variation, we then analyzed the joint effects of April T_{max} and June-July T_{max} on RWI for each
438 chronology independently using the base `lm()` function in R. Slopes and p-values for each
439 chronology are given in SI Table 1.

440 **Acknowledgements**

441 We gratefully acknowledge all researchers who assisted with data collection in the field and
442 laboratory, particularly Tsun Fung Au, Joshua Bregy, James Dickens, Karen Heeter, Anna
443 Hennage, Daniel King, James McGee, Benjamin Lockwood, Jennifer McGarvey, Victoria
444 Meakem, Josh Oliver, Jessica Shue, Karly Schmidt-Simard, Brandon Strange, Alyssa Terrell,
445 Brynn Taylor, Michael Thornton, Senna Robeson, Matt Wenzel, and Luke Wylie. Thanks to
446 David A. Orwig and members of the ForestGEO Ecosystems & Climate Lab at SCBI for helpful
447 feedback. The research was funded by ForestGEO (Smithsonian). Collection of tree-ring
448 samples was funded by a USDA Agriculture and Food Research Initiative grant 2017-67013-
449 26191 and from the Indiana University Vice Provost for Research Faculty Research Program.

450 **Author Contributions**

451 Cameron Dow and Kristina J. Anderson-Teixeira conceived the ideas and designed the study;
452 Cameron Dow, Loïc D'Orangeville, Erika B. Gonzalez-Akre, Ryan Helcoski, Grant L. Harley,

453 Justin T. Maxwell, Ian R. McGregor, William McShea, Neil Pederson, Alan J. Tepley, and
454 Kristina J. Anderson-Teixeira collected or oversaw collection of data; Cameron Dow, Albert Y.
455 Kim, Valentine Herrmann, Justin T. Maxwell, Ian R. McGregor, Sean McMahon analyzed the
456 data or provided analytical tools; Cameron Dow and Kristina J. Anderson-Teixeira led the
457 writing of the manuscript. All authors contributed critically to the drafts and gave final
458 approval for publication.

459 **Additional Information**

460 **Supplementary Information** is available for this paper.

461 Correspondence and requests for materials should be addressed to Kristina Anderson-Teixeira
462 (teixeirak@si.edu).

463 **References**

- 464 1. Jeong, S.-J., Ho, C.-H., Gim, H.-J. & Brown, M. E. Phenology shifts at start vs. End of
465 growing season in temperate vegetation over the Northern Hemisphere for the period
466 1982. *Global Change Biology* **17**, 2385–2399 (2011).
- 467 2. Keenan, T. F. *et al.* Net carbon uptake has increased through warming-induced changes in
468 temperate forest phenology. *Nature Climate Change* **4**, 598–604 (2014).
- 469 3. Buermann, W. *et al.* Widespread seasonal compensation effects of spring warming on
470 northern plant productivity. *Nature* **562**, 110–114 (2018).
- 471 4. Finzi, A. C. *et al.* Carbon budget of the Harvard Forest Long-Term Ecological Research
472 site: Pattern, process, and response to global change. *Ecological Monographs* **90**, e01423
473 (2020).
- 474 5. Stuble, K. L., Bennion, L. D. & Kuebbing, S. E. Plant phenological responses to
475 experimental warming: A synthesis. *Global Change Biology* **27**, 4110–4124 (2021).

- 476 6. Delgado, M. del M. *et al.* Differences in spatial versus temporal reaction norms for spring
477 and autumn phenological events. *Proceedings of the National Academy of Sciences* 202002713
478 (2020) doi:10.1073/pnas.2002713117.
- 479 7. Menzel, A. & Fabian, P. Growing season extended in Europe. *Nature* **397**, 659–659 (1999).
- 480 8. Menzel, A. *et al.* European phenological response to climate change matches the warming
481 pattern. *Global Change Biology* **12**, 1969–1976 (2006).
- 482 9. Ibáñez, I. *et al.* Forecasting phenology under global warming. *Philosophical Transactions of*
483 *the Royal Society B: Biological Sciences* **365**, 3247–3260 (2010).
- 484 10. Keeling, C. D., Chin, J. F. S. & Whorf, T. P. Increased activity of northern vegetation
485 inferred from atmospheric CO₂ measurements. *Nature* **382**, 146–149 (1996).
- 486 11. Dragoni, D. *et al.* Evidence of increased net ecosystem productivity associated with a
487 longer vegetated season in a deciduous forest in south-central Indiana, USA. *Global*
488 *Change Biology* **17**, 886–897 (2011).
- 489 12. Crabbe, R. A. *et al.* Extreme warm temperatures alter forest phenology and productivity
490 in Europe. *Science of The Total Environment* **563–564**, 486–495 (2016).
- 491 13. Zhou, S. *et al.* Explaining inter-annual variability of gross primary productivity from
492 plant phenology and physiology. *Agricultural and Forest Meteorology* **226–227**, 246–256
493 (2016).
- 494 14. Fu, Z. *et al.* Maximum carbon uptake rate dominates the interannual variability of global
495 net ecosystem exchange. *Global Change Biology* **25**, 3381–3394 (2019).
- 496 15. Xue, B.-L. *et al.* Global patterns of woody residence time and its influence on model
497 simulation of aboveground biomass. *Global Biogeochemical Cycles* **31**, 821–835 (2017).
- 498 16. Russell, M. B. *et al.* Residence Times and Decay Rates of Downed Woody Debris
499 Biomass/Carbon in Eastern US Forests. *Ecosystems* **17**, 765–777 (2014).
- 500 17. Zani, D., Crowther, T. W., Mo, L., Renner, S. S. & Zohner, C. M. Increased growing-
501 season productivity drives earlier autumn leaf senescence in temperate trees. *7* (2020).
- 502 18. Ahlström, A., Schurgers, G., Arneth, A. & Smith, B. Robustness and uncertainty in
503 terrestrial ecosystem carbon response to CMIP5 climate change projections. *Environmental*
504 *Research Letters* **7**, 044008 (2012).
- 505 19. Pan, Y. *et al.* A Large and Persistent Carbon Sink in the World's Forests. *Science* **333**, 988–
506 993 (2011).
- 507 20. Friedlingstein, P. *et al.* Global Carbon Budget 2020. *Earth System Science Data* **12**, 3269–
508 3340 (2020).

- 509 21. Pugh, T. A. M. *et al.* Role of forest regrowth in global carbon sink dynamics. *Proceedings of*
510 *the National Academy of Sciences* **116**, 4382–4387 (2019).
- 511 22. Arora, V. K. *et al.* Carbon concentration and carbon climate feedbacks in CMIP6 models
512 and their comparison to CMIP5 models. *Biogeosciences* **17**, 4173–4222 (2020).
- 513 23. Keenan, T. F. & Richardson, A. D. The timing of autumn senescence is affected by the
514 timing of spring phenology: Implications for predictive models. *Global Change Biology* **21**,
515 2634–2641 (2015).
- 516 24. Zohner, C. M., Renner, S. S., Sebald, V. & Crowther, T. W. How changes in spring and
517 autumn phenology translate into growth—experimental evidence of asymmetric effects.
518 *Journal of Ecology* **109**, 2717–2728 (2021).
- 519 25. D’Orangeville, L. *et al.* Peak radial growth of diffuse-porous species occurs during
520 periods of lower water availability than for ring-porous and coniferous trees. *Tree*
521 *Physiology* (2021) doi:[10.1093/treephys/tpab101](https://doi.org/10.1093/treephys/tpab101).
- 522 26. D’Orangeville, L. *et al.* Drought timing and local climate determine the sensitivity of
523 eastern temperate forests to drought. *Global Change Biology* **24**, 2339–2351 (2018).
- 524 27. Helcoski, R. *et al.* Growing season moisture drives interannual variation in woody
525 productivity of a temperate deciduous forest. *New Phytologist* **223**, 1204–1216 (2019).
- 526 28. McMahon, S. M. & Parker, G. G. A general model of intra-annual tree growth using
527 dendrometer bands. *Ecology and Evolution* **5**, 243–254 (2015).
- 528 29. Parmesan, C. & Yohe, G. A globally coherent fingerprint of climate change impacts across
529 natural systems. *Nature* **421**, 37–42 (2003).
- 530 30. Friedl, M. A. *et al.* A tale of two springs: Using recent climate anomalies to characterize
531 the sensitivity of temperate forest phenology to climate change. *Environmental Research*
532 *Letters* **9**, 054006 (2014).
- 533 31. Fu, Y. S. H. *et al.* Variation in leaf flushing date influences autumnal senescence and next
534 year’s flushing date in two temperate tree species. *Proceedings of the National Academy of*
535 *Sciences* **111**, 7355–7360 (2014).
- 536 32. Zhang, J. *et al.* Drought limits wood production of *Juniperus przewalskii* even as growing
537 seasons lengthens in a cold and arid environment. *CATENA* **196**, 104936 (2021).
- 538 33. Vicente-Serrano, S. M., Beguería, S. & López-Moreno, J. I. A Multiscalar Drought Index
539 Sensitive to Global Warming: The Standardized Precipitation Evapotranspiration Index.
540 *Journal of Climate* **23**, 1696–1718 (2010).
- 541 34. Zohner, C. M. & Renner, S. S. Ongoing seasonally uneven climate warming leads to
542 earlier autumn growth cessation in deciduous trees. *Oecologia* **189**, 549–561 (2019).

- 543 35. Xie, Y., Wang, X., Wilson, A. M. & Silander, J. A. Predicting autumn phenology: How
544 deciduous tree species respond to weather stressors. *Agricultural and Forest Meteorology*
545 **250–251**, 127–137 (2018).
- 546 36. Cuny, H. E. *et al.* Woody biomass production lags stem-girth increase by over one month
547 in coniferous forests. *Nature Plants* **1**, 15160 (2015).
- 548 37. Tardif, J. C. & Conciatori, F. Influence of climate on tree rings and vessel features in red
549 oak and white oak growing near their northern distribution limit, southwestern Quebec,
550 Canada. *Canadian Journal of Forest Research* **36**, 2317–2330 (2006).
- 551 38. Roibu, C.-C. *et al.* The Climatic Response of Tree Ring Width Components of Ash
552 (*Fraxinus excelsior* L.) And Common Oak (*Quercus robur* L.) From Eastern Europe.
553 *Forests* **11**, 600 (2020).
- 554 39. Kern, Z. *et al.* Multiple tree-ring proxies (earlywood width, latewood width and $\delta^{13}C$)
555 from pedunculate oak (*Quercus robur* L.), Hungary. *Quaternary International* **293**, 257–267
556 (2013).
- 557 40. Trumbore, S., Gaudinski, J. B., Hanson, P. J. & Southon, J. R. Quantifying ecosystem-
558 atmosphere carbon exchange with a ^{14}C label. *Eos, Transactions American Geophysical*
559 *Union* **83**, 265–268 (2002).
- 560 41. Richardson, A. D. *et al.* Seasonal dynamics and age of stemwood nonstructural
561 carbohydrates in temperate forest trees. *New Phytologist* **197**, 850–861 (2013).
- 562 42. Oishi, A. C. *et al.* Warmer temperatures reduce net carbon uptake, but do not affect water
563 use, in a mature southern Appalachian forest. *Agricultural and Forest Meteorology* **252**, 269–
564 282 (2018).
- 565 43. Kannenberg, S. A. *et al.* Linking drought legacy effects across scales: From leaves to tree
566 rings to ecosystems. *Global Change Biology* **25**, 2978–2992 (2019).
- 567 44. Gessler, A., Bottero, A., Marshall, J. & Arend, M. The way back: Recovery of trees from
568 drought and its implication for acclimation. *The New phytologist* **228**, 1704–1709 (2020).
- 569 45. Fisichelli, N. A., Frelich, L. E. & Reich, P. B. Temperate tree expansion into adjacent boreal
570 forest patches facilitated by warmer temperatures. *Ecography* **37**, 152–161 (2014).
- 571 46. Anderson-Teixeira, K. J. *et al.* Joint effects of climate, tree size, and year on annual tree
572 growth derived from tree-ring records of ten globally distributed forests. *Global Change*
573 *Biology* **n/a**, (2021).
- 574 47. Banbury Morgan, R. *et al.* Global patterns of forest autotrophic carbon fluxes. *Global*
575 *Change Biology* gcb.15574 (2021) doi:[10.1111/gcb.15574](https://doi.org/10.1111/gcb.15574).

- 576 48. Churkina, G., Schimel, D., Braswell, B. H. & Xiao, X. Spatial analysis of growing season
577 length control over net ecosystem exchange. *Global Change Biology* **11**, 1777–1787 (2005).
- 578 49. Bourg, N. A., McShea, W. J., Thompson, J. R., McGarvey, J. C. & Shen, X. Initial census,
579 woody seedling, seed rain, and stand structure data for the SCBI SIGEO Large Forest
580 Dynamics Plot: *Ecological Archives* E094-195. *Ecology* **94**, 2111–2112 (2013).
- 581 50. Anderson-Teixeira, K. J. *et al.* CTFS-ForestGEO : A worldwide network monitoring
582 forests in an era of global change. *Global Change Biology* **21**, 528–549 (2015).
- 583 51. Davies, S. J. *et al.* ForestGEO: Understanding forest diversity and dynamics through a
584 global observatory network. *Biological Conservation* **253**, 108907 (2021).
- 585 52. Friedl, M., Gray, J. & Sulla-Menashe, D. MCD12Q2 MODIS/Terra+Aqua Land Cover
586 Dynamics Yearly L3 Global 500m SIN Grid V006. (2019)
587 doi:[10.5067/MODIS/MCD12Q2.006](https://doi.org/10.5067/MODIS/MCD12Q2.006).
- 588 53. Anderson-Teixeira, K. *et al.* Forestgeo/Climate: Initial release. (2020)
589 doi:[10.5281/ZENODO.4041609](https://doi.org/10.5281/ZENODO.4041609).
- 590 54. Benestad, R. E., Hanssen-Bauer, I. & Chen, D. *Empirical-statistical downscaling*. (World
591 Scientific Pub Co Inc, 2008).
- 592 55. Boose, E. & Gould, E. Shaler Meteorological Station at Harvard Forest 1964-2002. (2021)
593 doi:[10.6073/PASTA/213335F5DAA17222A738C105B9FA60C4](https://doi.org/10.6073/PASTA/213335F5DAA17222A738C105B9FA60C4).
- 594 56. Boose, E. Fisher Meteorological Station at Harvard Forest since 2001. (2021)
595 doi:[10.6073/PASTA/69E92642B512897032446CFE795CFFB8](https://doi.org/10.6073/PASTA/69E92642B512897032446CFE795CFFB8).
- 596 57. van de Pol, M. *et al.* Identifying the best climatic predictors in ecology and evolution.
597 *Methods in Ecology and Evolution* **7**, 1246–1257 (2016).
- 598 58. Gabry, J. *et al.* Rstanarm: Bayesian Applied Regression Modeling via Stan. (2020).
- 599 59. Stan_Development_Team. Stan Modeling Language Users Guide and Reference Manual,
600 2.28. (2019).
- 601 60. Beguería, S., Vicente-Serrano, S. M., Reig, F. & Latorre, B. Standardized precipitation
602 evapotranspiration index (SPEI) revisited: Parameter fitting, evapotranspiration models,
603 tools, datasets and drought monitoring. *International Journal of Climatology* **34**, 3001–3023
604 (2014).
- 605 61. Vicente-Serrano, S. M., Beguería, S. & López-Moreno, J. I. A Multiscalar Drought Index
606 Sensitive to Global Warming: The Standardized Precipitation Evapotranspiration Index.
607 *Journal of Climate* **23**, 1696–1718 (2010).
- 608 62. Stokes, M. A. & Smiley, T. L. *An Introduction to Tree-ring Dating*. (University of Arizona
609 Press, 1968).

- 610 63. Alexander, M. R. *et al.* The potential to strengthen temperature reconstructions in
611 ecoregions with limited tree line using a multispecies approach. *Quaternary Research* **92**,
612 583–597 (2019).
- 613 64. Dye, A. *et al.* Comparing tree-ring and permanent plot estimates of aboveground net
614 primary production in three eastern U.S. forests. *Ecosphere* **7**, e01454 (2016).
- 615 65. Maxwell, J. T. *et al.* Sampling density and date along with species selection influence
616 spatial representation of tree-ring reconstructions. *Climate of the Past* **16**, 1901–1916 (2020).
- 617 66. *Methods of Dendrochronology: Applications in the Environmental Sciences*. (Springer
618 Netherlands, 1990). doi:[10.1007/978-94-015-7879-0](https://doi.org/10.1007/978-94-015-7879-0).
- 619 67. Cook, E. R. A Time Series Analysis Approach to Tree Ring Standardization. vol. PhD
620 (University of Arizona, 1985).
- 621 68. Cook, E. R. & Peters, K. Calculating unbiased tree-ring indices for the study of climatic
622 and environmental change. *The Holocene* **7**, 361–370 (1997).
- 623 69. Jones, P. D., Osborn, T. J. & Briffa, K. R. Estimating sampling errors in large-scale
624 temperature averages. *Journal of Climate* **10**, 2548–2568 (1997).
- 625 70. Harris, I., Osborn, T. J., Jones, P. & Lister, D. Version 4 of the CRU TS monthly high-
626 resolution gridded multivariate climate dataset. *Scientific Data* **7**, (2020).
- 627 71. Bunn, A. G. A dendrochronology program library in R (dplR). *Dendrochronologia* **26**, 115–
628 124 (2008).
- 629 72. Zang, C. & Biondi, F. Dendroclimatic calibration in R: The bootRes package for response
630 and correlation function analysis. *Dendrochronologia* **31**, 68–74 (2013).
- 631 73. Biondi, F. & Waikul, K. DENDROCLIM2002 : A C++ program for statistical calibration of
632 climate signals in tree-ring chronologies. *Computers & Geosciences* **30**, 303–311 (2004).

Supplementary Files

This is a list of supplementary files associated with this preprint. Click to download.

- [DowSITable1.xlsx](#)
- [DowExtendedData.pdf](#)